RL-75-066
Copy 2

NEW DEVELOPMENTS IN THE MAGNET DESIGN COMPUTER PROGRAM GFUN

A G A M Armstrong, C J Collie, N J Diserens, M J Newman,
J Simkin, C W Trowbridge.

Presented at the 5th International Conference on Magnet Technology,
Frascati, Rome, 1975.

Computing Applications Group
Applied Physics Division
Rutherford Laboratory
Chilton, Didcot, Oxon, OX11 0QX

RL-75-066

March 1975

CONTENTS

NEW DEVELOPMENTS IN THE MAGNET DESIGN COMPUTER PROGRAM GFUN3D

A G A M Armstrong, C J Collie, N J Diserens, M J Newman, J Simkin, C W Trowbridge
Rutherford Laboratory
Chilton, Didcot, Oxon, OX11 0QX, England.

SUMMARY

The GFUN system for designing magnets was first presented at the 4th Conference of this series at Brookhaven in September 1972. Since that time several major improvements have been introduced which have extended the scope and power of the three dimensional program. In this system the contribution to the magnetic field for conductor regions is determined by direct integration, thus enabling the contribution from the non-linear iron regions to be expressed as the solution of an integral equation. For this purpose the iron is subdivided into a large number of triangular prisms.

The improvements include a number of new conductor geometries suitable for saddle coil and more conventional windings; an increase in the practical limit of the number of elements which can be used to represent saturable iron; the extension to higher order symmetries, both multipole and rotational, thus achieving economies in the number of elements that have to be specified.

The introduction of backing store methods for the solution of the large set of algebraic equations required in the magnetisation computation has resulted in a more efficient use of the computer.

Higher level facilities such as particle tracking and computation of field integrals have been implemented to aid in the solution of particular problems.

Several comparisons of calculated fields with measurements are given including a detailed study of the Harwell Variable Energy Cyclotron.

1. INTRODUCTION.

The 'GFUN' computer program for the analysis of magnetic fields was developed at the Rutherford Laboratory and some preliminary results were reported at Brookhaven in 1972.[1]

The program utilises graphics techniques and for a large class of problem is fully user interactive. The computational method used to determine the magnetic field for a given magnet structure is based on an integral equation formulation for the unknown magnetisation (dipole strength and direction per unit volume). In this method only the regions of saturable material need to be discretized and the requirements of prescribed boundaries are avoided. The contribution to the resultant magnetic field at any point from conductor regions is obtained by direct integration. The mathematical details and the advantages and disadvantages have been discussed in previous papers.[1,2,3,4]

The aim of this report is (a) to review the various major improvements that have been incorporated into the program since 1972; (b) to present results comparing the program with measured magnets and magnets analysed with the TRIM program; (c) to discuss the limitations of the program, the work in progress and future ideas which may extend the scope of the program.

2. DEVELOPMENTS SINCE THE 1972 BROOKHAVEN CONFERENCE

2.1 Coil Geometries. To compute the magnetic field produced by coils a filament integration technique is normally used. The path of filaments in a section of coil is described by parametric equations and a numeric integration of the field from finite straight filaments is performed along the path. The path is subdivided until a given accuracy is reached. The field from the filamentary currents is then integrated over the cross section of the coil.[5,6] Field integrals are computed in the same way. Analytic integrations are used whenever possible.

The shape of a coil is defined by an end code and the minimum number of parameters. Each coil is continuous and is built up from an assembly of basic shapes such as straights, arcs and helices of rectangular or sector cross section.

At present the following coils can be used:

(1) Solenoids.

(2) Racetracks - one quadrant comprising a straight, 90° arc and a further straight.

(3) Windings consisting of parallel z-directed straights connected by:

(a) bedstead ends
(b) helices and an arc (5)
(c) an approximate constant perimeter end (5,7)

The existing shapes may be combined or new shapes and coils may be added without difficulty. For example see Figure 2.1 for the geometry and magnetic fields in a toroidal system of coils of D shaped cross section. In this case a special program has been written to generate geometry, field and force data. This pre-program is then used in conjunction with the Finite Element Stress Program FINESSE. (8)

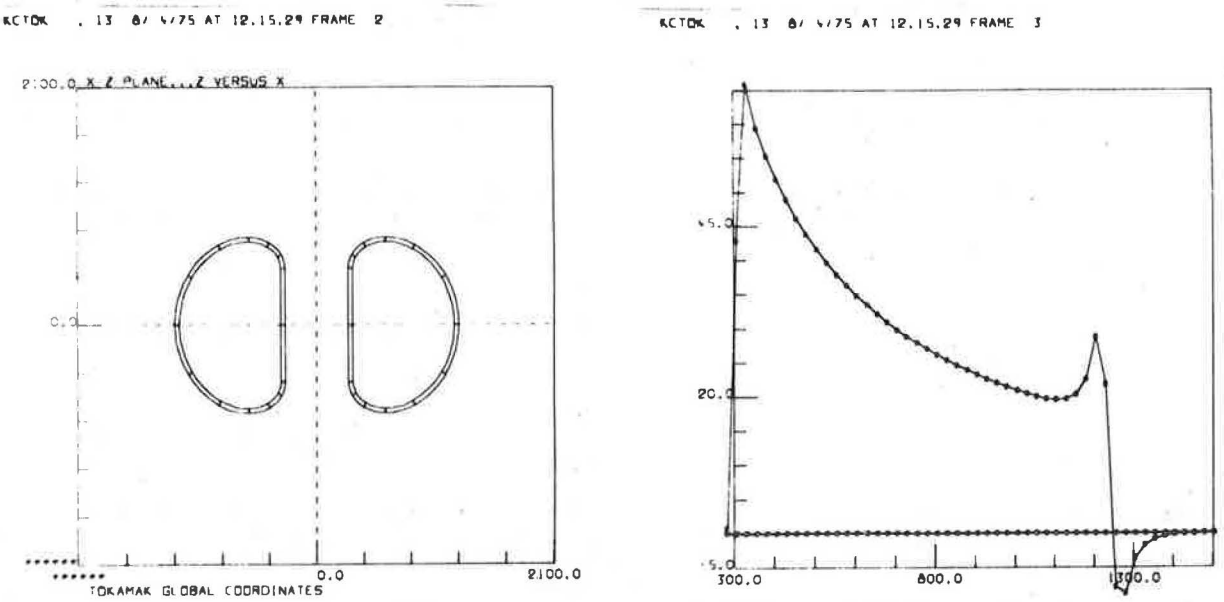

Radial cross section

B_θ (kilogauss) field as a function of radius

FIG. 2.1 - TOKAMAK COILS

2.2 Coil Symmetries. The coils can have any order multipole symmetry produced by rotation about the z axis or reflection in planes containing the z axis. With low order symmetries, eg. that required for a 'C' magnet, the coils can be displaced and rotated to any position in the xy plane. Solenoids can be displaced to any position in the xy plane and may also have their axes inclined to the z axis in an zx plane.

2.3 Improved Methods of Solving Non-Linear Equations.

2.3.1 General. In order to find the three components of field at the centroid of each iron element, it is necessary to solve the large set of simultaneous non-linear equations:

$$AH = - H_c \qquad (1)$$

where H is the column matrix of field components at the centroid, H_c is the column matrix of field components due to conductors alone, and A is a dense matrix whose coefficients depend on the geometry and on the values of H.

Equation (1) can be solved by treating it as a quasi-linear problem and using the iteration:

$$H^{k+1} = - A^{-1}(H^k) . H_c$$

It is found that this does converge in almost all cases. There are three main disadvantages:

(a) All existing routines that could be found for solving linear equations with dense matrices assumed that the order was low enough for the whole matrix to be stored in main memory. This limited the number of elements that could be used to represent the iron geometry.

(b) Iterations only have linear terminal convergence.

(c) Iterations do not have guaranteed convergence.

2.3.2 Use of Backing Store to Solve Linear Problems. A package of Fortran routines has been written for solving linear problems with dense matrices using direct access backing storage (disc) to store the complete matrix while only a fraction of this is held in main memory at any time.[9] The method is Gaussian Elimination and Back Substitution, with incomplete partial pivoting. The matrix is partitioned into a square set of square sub-matrices, N in number, each of which is called a block. The total number of times that the disc is accessed is:

$$\frac{1}{6}(8\,N^{3/2} - 3N + 13N^{1/2} - 54).$$

Four blocks are in core at any time.

In the elimination stage, row pivoting is performed to bring the largest coefficient in each column to the pivotal position. The pivoting is incomplete because only the diagonal block and the block immediately below it in the matrix will be in main memory when the column is searched. In practice, since the order of the block matrix is 90, it is unlikely that the largest coefficient amongst the 90 to 180 present will be significantly smaller than the largest in the whole column.

The precision of the algorithm is somewhere between single and double precision (32 bit and 64 bit).

This package has been tested on matrices of order up to 600 which needs N = 49 blocks. The processor time on the Rutherford Laboratory IBM 360/195 to solve such a linear problem is 1.25 mins. and the elapsed time is 6.3 mins. average. The amount of main memory used is 510 Kbytes. If the whole matrix were stored in main memory, the program would occupy 1.5 Mbytes.

2.3.3 Secant Method for Quadratic Terminal Convergence. A package of Fortran routines has been written for solving large sets of non-linear equations using the secant method, which uses the backing store package to solve the linear sub-problem.[10]

Re-arrange equation (1) to get:

$$F(H) = AH + H_c$$

where $F(H) = 0$ at the solution. The secant iteration is then:

$$H^{k+1} = H^k - J^{-1}(H^k, h^k).F(H^K)$$

where J is the approximation to the Jacobian of F, h is the vector step length.

There is a major saving in computation over that needed for a general function, since each term in the Jacobian depends on only three unknowns. Hence the number of function evaluations to calculate the Jacobian is only 4 instead of n+1.

This iteration has guaranteed quadratic convergence as the solution is approached. However, it suffers from the usual disadvantage of all such methods, that it is unstable unless the initial estimate of the solution is sufficiently 'close' to the true solution.

This package is now used and is very effective when this condition is fulfilled.

2.3.4 Guaranteed Convergence. It is planned to implement an algorithm which hopefully will give both guaranteed convergence from any starting point and fast terminal convergence (see Section 7.2).

From a guessed uniform field, simple stable iterations are used until partial convergence is achieved. The program then switches to the secant method. If this converges the solution is found. If it does not converge after two iterations, the program switches back to the stable method. After a number of further iterations, the secant method is tried again. This is an 'ad-hoc' procedure since no reliable criterion has been found for deciding when it is safe to switch to the secant method. However, the total computing time to solve a large problem can be substantially reduced.

2.4 Direct Access Filing System. The data defining magnet models which have been prepared with GFUN can be stored as files on an attached disc dataset. A new Fortran routine removes the previous restriction on the maximum number of files, and enables the user to list only those files whose names begin with a given pair of letters.

2.5 Particle Beam Tracking. In order to simulate the performance of any proposed magnet when used as a focussing or particle handling device a facility for tracking rays and beams of charged particles has been incorporated into GFUN3D. The procedure adopted is a direct solution of the equations of motion using a 4th order Runge Kutta method. There are no field approximations used - the named field option 'GETB' is invoked to calculate the field components at any point. Figure 2.5 demonstrates the use of this facility for a magnet system, proposed for use in radiation therapy in hospitals, in which a particle beam is bent through two non-coplanar right angles.

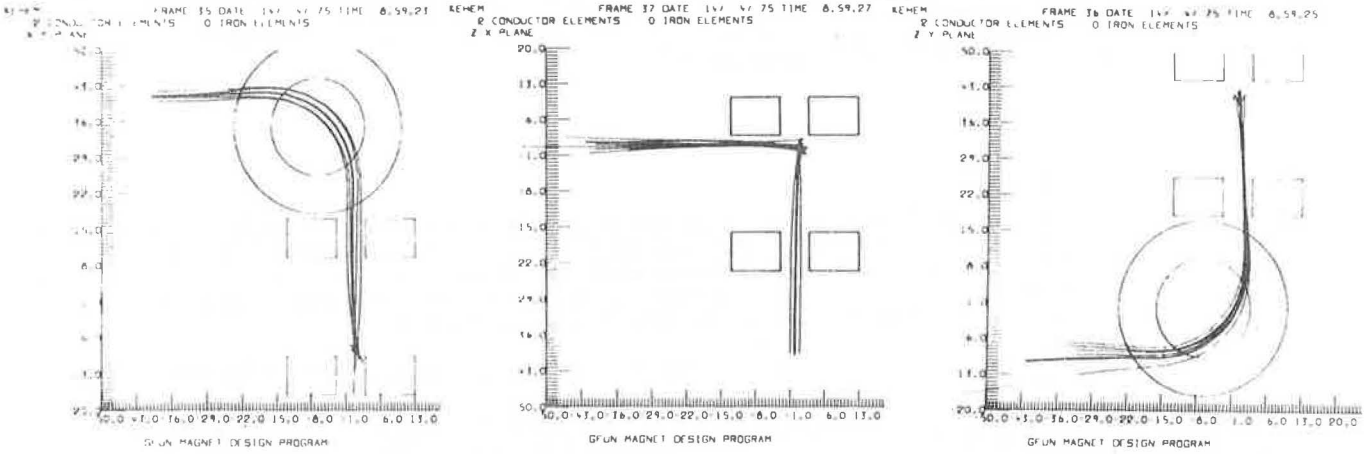

FIG. 2.5 - PARTICLE TRACKING FACILITY

2.6 Iron Elements. To cure some problems found when computing low field, iron dominated magnets the prisms can be orientated in any direction - see Section 5.

Only the minimum amount of material is subdivided; every element has a symmetry code and this is used to generate a set of elements that are related to the first by rotation or reflection about a symmetry line or plane. The symmetry code implies a correspondence between the magnetisations of the set of elements. The magnitude is the same in all elements of the set. However if a local coordinate system is rotated or reflected with the element, the magnetisation components will have their signs changed appropriately.

As an example, for a quadrupole focussing magnet the symmetry code for the iron and conductors would be 4. The iron and coils would then be defined in the positive z direction between 0° and 45° in the xy plane. The other 15 parts are implied by the symmetry code. To solve for the magnetisations the coupling coefficients for the other 15 parts to all elements in the first octant are calculated. The coefficients with suitable sign changes and transformations are then included with the coefficients for equivalent elements in the first part.

For magnets that consist of widely separated and therefore almost independent volumes of iron a technique has been used whereby the magnetisation of one volume is held constant whilst those in another volume are computed. This has proved useful when computing the effect of mirror plates and in certain cases for refining an initially crude solution over a small volume. The fields from elements that are held constant are added to the field from the coils in order to compute the magnetisation of the other volume. In cases with stronger coupling it may be necessary alternately to hold and release the magnetisation of each volume in order to converge on a good solution.

3. COMPARISONS WITH MEASUREMENT

3.1 The Harwell Variable Energy Cyclotron Magnet. The magnet is basically a simple 'pot core' design with spiral ridges and edge shims to shape the field for particle focussing. Accurate field surveys were made at many field levels.[11] In Figures 3.1.1 to 3.1.3 the model used with GFUN is shown. The real magnet has a pole with three-fold symmetry and a yoke with two-fold symmetry. The yoke does not saturate and produces little field asymmetry in the gap. In the computer model a three-fold symmetry yoke was used to economise on the number of iron elements. Two hundred iron elements were used.

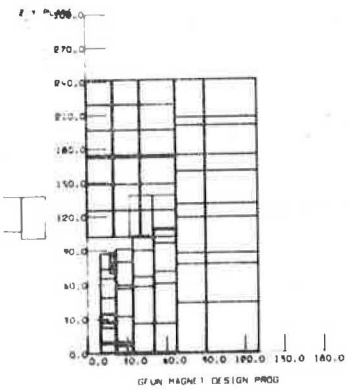

FIG. 3.1.1 - Z-Y PLANE

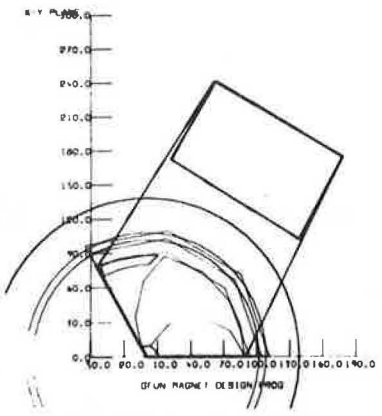

FIG. 3.1.2 - X-Y PLANE

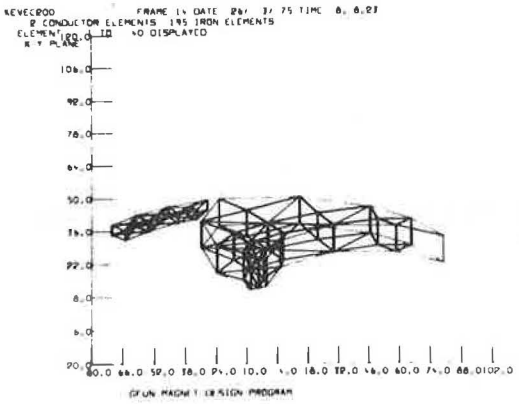

FIG. 3.1.3 - PERSPECTIVE VIEW OF SPIRAL RIDGE HARWELL VARIABLE ENERGY CYCLOTRON MAGNET

The gap field was analysed into circular harmonics at various radii (R cms) measured from the centre of the pole. The series used was:

$$H_z = H_o(1 + A_3\text{Cos}3\theta + B_3\text{Sin}3\theta + A_6\text{Cos}6\theta + B_6\text{Sin}6\theta \ldots\ \text{etc.})$$

where:

H_z is the axial field in gauss

H_o is the steady field in gauss at radius R

θ is the azimuthal angle

$A_n B_n$ are the harmonic coefficients.

The important field parameters are the magnitude of H_o, and the values of A_n and B_n and the way they change as functions of radius. Calculated and measured values are tabulated here. (Table 3.1)

The computed values of H_o have the correct behaviour as a function of radius but they are approximately 6% low. This is caused by there being too few iron elements in the yoke. Using many elements to define the pole geometry has however reproduced the field shape very well. The higher order harmonics when normalised to the steady fields - H_o - agree to better than 1% of H_o.

TABLE 3.1-MEASURED AND COMPUTED HARMONIC COEFFICIENTS OF THE VEC, AT A CURRENT OF 1200 AMPS

Radius cms	25.4		38.1		50.8		63.5		76.2		88.9	
Order of Harmonic	Mea-sured	Com-puted	Mea-sured	Com-puted	Mea-sured	Com-puted	Mea-sured	Com-puted	Mea-sured	Com-puted	Mea-sured	Com-puted
H_o (gauss)	8767.	7900.	8586.	7880.	8599.	7950.	8755.	8150.	8966.	8370.	7552.	6700.
A_3	-.2542	-.2540	-.2660	-.2580	-.1712	-.1588	-.0156	-.0148	.1350	.1415	.1900	.1830
B_3	.0924	.1040	.2263	.2380	.3353	.3410	.3699	.3683	.3067	.3104	.2044	.1900
A_6	-.0058	-.0038	0.0	.0012	.0330	.0314	.0748	.0650	.0566	.0650	-.0166	-.0060
B_6	.0076	.0030	.0252	.0200	.0337	.0280	.0036	.0050	-.0794	-.0680	-.0900	-.0970
A_9	.0072	.0058	-.0179	-.0209	-.0495	-.0550	-.0122	-.0190	.0250	.0300	.0169	.0090
B_9	-.0122	-.0140	-.0310	-.0260	.0047	.0107	.0459	.0422	.0154	.0090	-.0028	-.0054

3.2 PEM C-Magnet. This example illustrates some of the improvements made to GFUN since 1972. At that time an attempt was made to calculate the C-Magnet which has a tapered cobalt pole-tip and other three-dimensional features, see Figures 3.2.1 to 3.2.4. The calculated central field was approximately 5% low - this discrepancy was attributed to certain limitations of the program at that time, including the inability to handle more than one material and more than 100 iron elements. These restrictions have now been removed and the calculated centre field is now within 0.2% of the measurements.

The magnet has now been modified to allow a beam of particles to enter a polarised target placed in the good field region under the pole. These modifications include a rectangular channel machined through the 'back return yoke'. Figure 3.2.5 shows a comparison of calculated fields with measurements for this revised configuration.[12] As can be seen there is a significant error in the shape of the field as a function of radius. This discrepancy is probably due to the poor representation of the pole-tip taper, using prism elements. It is hoped to do further comparisons of calculations with measurements when the tetrahedral element is available, see Section 5.

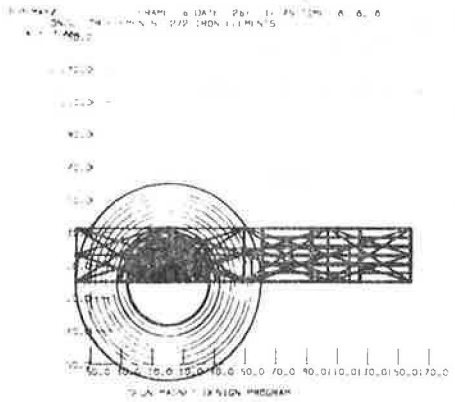

FIG. 3.2.1 - X-Y PLANE

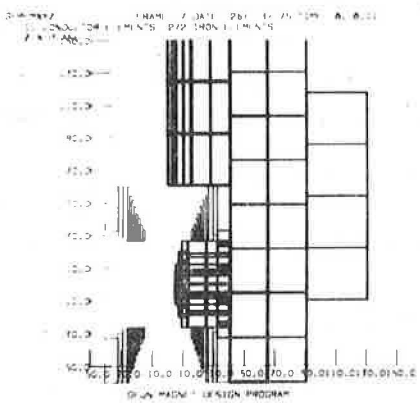

FIG. 3.2.2 - Z-X PLANE

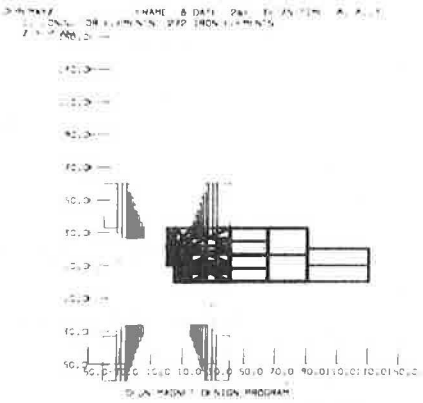

FIG. 3.2.3 - Z-Y PLANE

PEM C-YOKE MAGNET

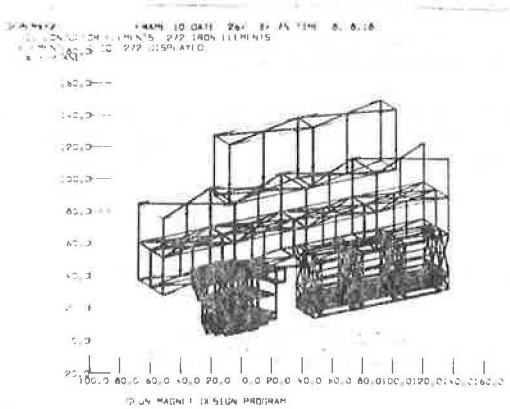

FIG. 3.2.4 - PERSPECTIVE VIEW OF PEM YOKE

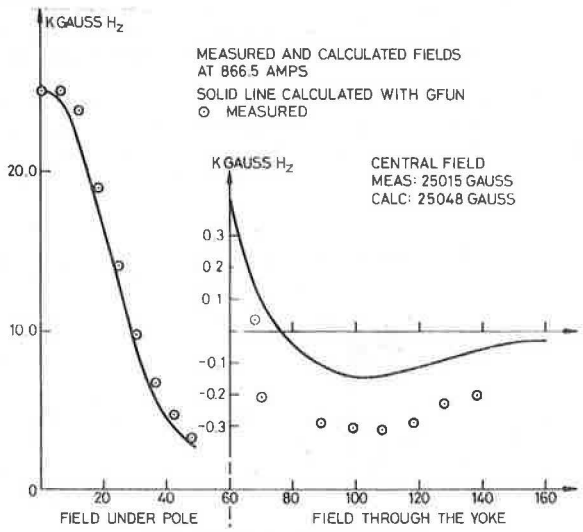

FIG. 3.2.5 - PEM RESULTS
PEM MAGNET MODIFIED

3.3 The Superconducting AC 5 Magnet. This is a superconducting dipole magnet designed for fast rise times and a maximum field of 5 T. A paper on the performance of this magnet appears in the Proceedings. Figs.3.3.1 & 2 show the computer generated pictures of this magnet from the GFUN program. The magnet was designed to produce a homogeneous field in the aperture, and the position of the end turns was optimised to give a homogeneous field integral through the magnet. The GFUN program was used to determine the iron dimensions such that saturation produced a minimal effect on the field quality and also to check the calculations on the position of the end windings.

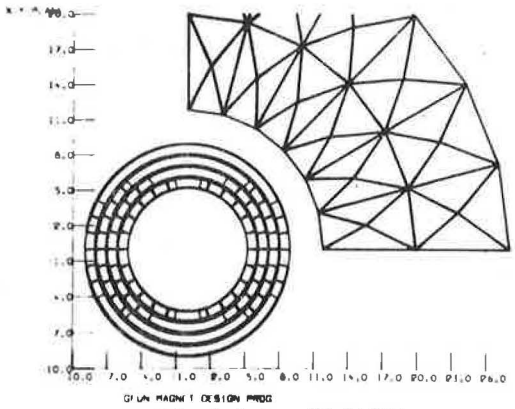

FIG. 3.3.1 - XY-PLANE

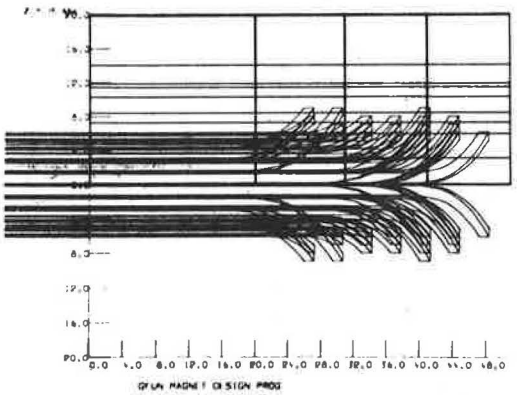

FIG. 3.3.2 - Z-Y PLANE

AC5 SUPERCONDUCTING DIPOLE MAGNET

In the aperture the central field and field integrals produced by the magnet are best described by a circular harmonic series of the type:

$$H_\theta = H_o \left[\sum_{n=1,3,5 \text{ etc}}^{\infty} A_n \left(\frac{r}{a}\right)^{n-1} \cos(n\theta) + B_n \left(\frac{r}{a}\right)^{n-1} \sin(n\theta) \right]$$

where:

H_θ is the azimuthal component of the field or field integral, a similar expression holds for H_r - the radial component

r is the radius in cms

a is the inside radius of the magnet coil in cms (= 5.23 cm)

θ is the azimuthal angle

A_n and B_n are the harmonic coefficients normalised to the inside radius of the coil

H_o is the central field or field integral.

The central field and field integral measurements at room temperature, for a coil with and without its iron shield are compared to the computed values in Table 3.3A. Only low field measurements were available at the time this report was written, and values of H_o had not been measured.

TABLE 3.3A -HARMONIC COEFFICIENTS OF THE AC 5 SUPERCONDUCTING DIPOLE MAGNET

ORDER OF THE HARMONIC	COIL ONLY				COIL WITH IRON YOKE			
	CENTRAL FIELD		FIELD INTEGRAL		CENTRAL FIELD		FIELD INTEGRAL	
	COMPUTED	MEASURED	COMPUTED	MEASURED	COMPUTED	MEASURED	COMPUTED	MEASURED
A_1	1.0	1.0	1.0	1.0	1.0	1.0	1.0	1.0
A_3	-.0071	-.0048	-.0068	-.0045	+.0006	.0019	-.0020	-.0003
A_5	0.0	-.0014	-.0014	-.0036	-.0001	-.0013	-.0011	-.0018
A_7	.0006	.0015	-.0011	.0024	.0004	.0015	-.0008	-.0002
A_9	-.0029	-.0032	-.0037	-.0104	-.0021	-.0039	-.0028	-.0020

Only the values of A_1, A_3 etc. are shown since these are the only coefficients possible in a perfect dipole. The results seem to agree very well and any errors are within those expected from the accuracy of the model.

It has also been possible to calculate the remanent fields produced by this superconducting coil. The coil can be infilled with 'iron' prisms which have a BH curve representing the weak diamagnetic behaviour of the superconductor. The magnitude of the diamagnetic effect is calculated as a function of H from measured critical currents. A solution for the magnetisation of the iron yoke and the diamagnetic coil can then be found. The central field is given approximately by a harmonic series of the form:

$$H_0 = H_1 \cos\theta + H_3 \left(\frac{r}{a}\right)^2 \cos 3\theta + H_5 \left(\frac{r}{a}\right)^4 \cos 5\theta \quad \text{etc.}$$

where

H_0 is the azimuthal component of the remanent field in gauss

H_1 etc are the magnitude of the harmonic components in gauss

r, a and θ as before.

Table 3.3B shows the measured and computed values of H_1 etc. The difference between the two H_1 coefficients is caused by the remanent field from the iron yoke which was not calculated. However the remanent field for the iron has been measured and is - 2.7 gauss.

TABLE 3.3B - REMANENT FIELDS PRODUCED BY THE AC5 SUPERCONDUCTING DIPOLE MAGNET

Harmonic coefficient	Computed	Measured
H_1	- 7.1	-11.2
H_3	-14.5	-14.95
H_5	3.90	+ 3.94
H_7	- 5.30	- 4.97
H_9	4.50	4.21

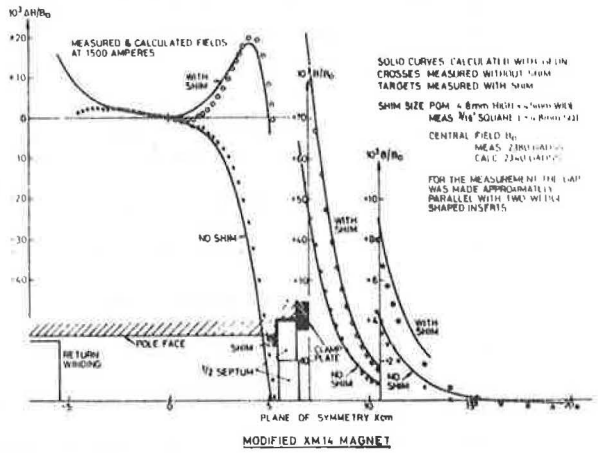

FIG. 3.4 - MODIFIED XM14 SEPTUM MAGNET

3.4 XM14 Septum Magnet. Part of the new Nimrod Hall 1 beam switchyard will use zero-gradient septum magnets; it may be possible to modify existing gradient septum magnets by providing them with parallel-gap yokes. Since the existing coils are not suited to this configuration, a considerable amount of computation is needed to establish the form which the correction devices will take. It seemed reasonable to check the program before starting these calculations, and to this end some simple measurements have been compared with computed fields. The gradient septum magnet XM14 was provided with wedge-shaped shims to make the gap approximately parallel, and powered at 1500 A. (It will eventually be operated at about 8000 A.) The field defect due to the oversize septum was partially compensated with a 3/16" square iron shim just behind the septum. Measured and calculated fields both with and without the square shims are displayed in Figure 3.4.

4. COMPARISONS WITH OTHER PROGRAMS

4.1 EPIC Prototype Dipole Magnet. The cross section of the prototype dipole magnet for the EPIC proposal[17] is shown in Fig.4.1a. The magnet will be 4.5 m effective length, with a laminated yoke of 96% Stacking Factor. Both GFUN and TRIM were used to find the sizes of pole-edge shims which would enlarge the good-field region. The results are summarised in Fig. 4.1b, both for the unshimmed and for the shimmed poles.[18] The agreement was considered satisfactory, so that a prototype magnet with this cross-section has been ordered and is due for delivery in August 1975.

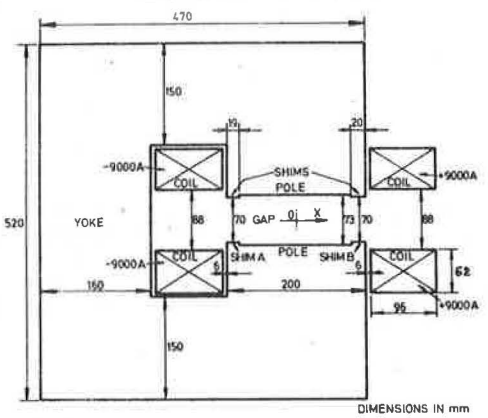

FIG. 4.1A NOMINAL DIPOLE MAGNET SECTION

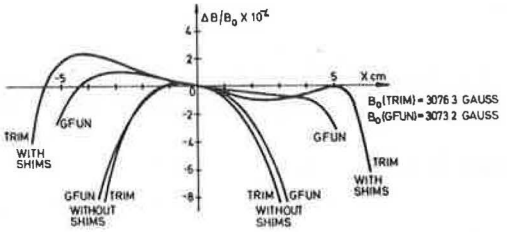

FIG. 4.1B CALCULATED FIELD ERROR $\Delta B/B_0$ FOR THE EPIC PROTOTYPE DIPOLE MAGNET. GFUN & TRIM RESULTS ARE SHEWN FOR THE FIELD ON THE MEDIAN PLANE (y=0)

4.2 Superconducting Dipole Magnet. The harmonic coefficients of an infinitely long four layer dipole coil, with constant current density, and a cylindrical constant permeability iron yoke, were calculated analytically. The magnet was very similar to the design shown in Section 3.3. The harmonic series used was as shown in Section 3.3. The harmonic coefficients were then computed using TRIM and a 2-dimensional limit in GFUN. The results for an iron yoke with permeability = 1000.0 are given below.

TABLE 4.2 - HARMONICS OF A FOUR LAYER DIPOLE WINDING WITH AN IRON SHIELD OF PERMEABILITY 1000.0

Order of the Harmonic	Analytic coefficients	TRIM coefficients	GFUN coefficients
H_o	1913.0	1914.0	1914.4
A_1	1.0	1.0	1.0
A_3	0.000020	0.000020	0.000026
A_5	-0.000090	-0.000110	-0.000090
A_7	0.000028	0.000036	0.000028
A_9	0.000003	-0.000003	0.000004
A_{11}	0.00189	0.00190	0.00189

96 iron elements were used to obtain the GFUN result and 9000 points were used for the TRIM run. GFUN took 60 secs.CPU and 400K; TRIM used 120 secs. CPU and 560K; both ran on the Rutherford Laboratory IBM 360/195.

5. LIMITATIONS OF THE PRESENT MODEL

5.1 Constant Magnetisation Assumption. In the present formulation of the magnetic field algorithm the magnetisation vector is assumed to be constant throughout the volume of a particular element. This constraint in turn means that the magnetisation is not continuous from one element to another which may result in a lack of smoothness in the results. One solution to this difficulty is to employ a sufficiently large number of elements. To determine what is sufficiently large needs careful consideration. Ideally the saturable regions should be magnetised successively for a range of element subdivisions until the change in computed field is less than the desired accuracy. For high accuracies, say less than 1% for genuine 3D magnet geometries, the level of subdividion may often exceed the capacity of the computer storage; eg the 220 element problem discussed in Section 3 required 2 Mbytes and 45 minutes of CPU on an IBM 360/195 computer. The alternative methods using backing store, outlined in Section 2.2, are aimed at reducing the memory requirements and should handle problems up to 400 elements before the elapse time becomes prohibitive. Thus 400 probably sets the upper limit for the number of constant magnetisation elements using current available computer hardware.

A better solution to this difficulty might be to remove the constraint of constant magnetisation by introducing a linear or higher order variation of magnetisation. A formulation using a linear variation has been worked out[15] and is currently under test for a range of simple problems. The results of these experiments demonstrates that the expected economy of elements can be achieved (up to a factor of 2 in 2D) for the same accuracy but much remains to be done before a working program becomes available using this technique. The extension of this idea to 3 dimensions using tetrehedral elements is discussed in Section 6.3.

5.2 Looping of Magnetisation Vectors. This phenomenon was first noticed during the use of the program to investigate the end effects of a conventional iron quadrupole.[21] It was subsequently rediscovered and the possible causes investigated by Ch Iselin at CERN.[19] The effect is best illustrated by an example; in Figures 5.1 and 5.2 are shown the resultant magnetisation patterns predicted by the program for two iron blocks placed in a uniform external field of 1.0 Kgauss. The lower permeability case (μ = 10) shows the expected pattern whereas in the higher permeability case (μ = 500) the vectors are 'looping'. The point at which looping appears is context dependent and in the example given here occurs for μ > 100.

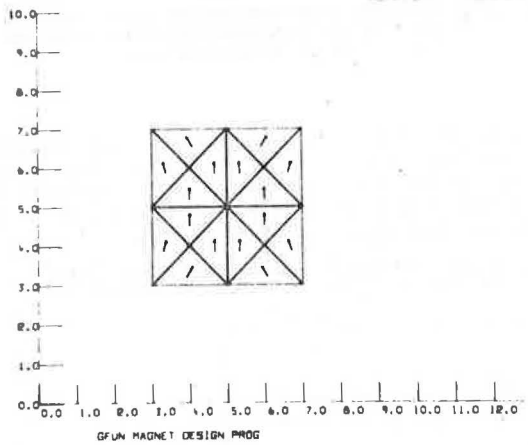

FIG. 5.1 - EXPECTED PATTERN

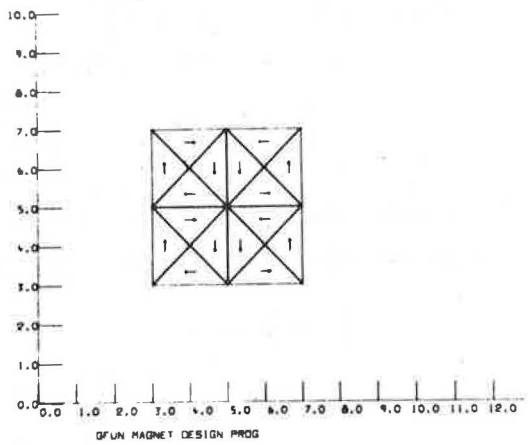

FIG. 5.2 - LOW-FIELD 'LOOPING'

MAGNETISATION VECTORS FOR BLOCKS IN UNIFORM EXTERNAL FIELD

A possible explanation of this effect arises from the near singular nature of the magnetisation coefficient matrix as the permeability becomes large. For example, if equation (2.3.1) is expressed in terms of the element coefficient matrix C[1]

viz: $(\chi C - I)H = -H_c$ (1)

where χ is the susceptibility and I the unit matrix. From (1) it would be expected that for large uniform χ that:

$$H \sim \frac{1}{\chi} \quad (2)$$

However in frequent cases this is not true, it has thus to be assumed that C is nearly singular.

Dividing by χ equation (1) becomes:

$$(C - \frac{I}{\chi}).\ H = (C - \lambda I).\ H = -\lambda H_c, \text{ where } \lambda = \frac{1}{\chi}$$

From this formulation it can be seen that as λ tends to zero, the equation tends to an eigenvalue problem and λ must approach an eigenvalue of C. Indeed, for a large class of problems, zero is an eigenvalue. Iselin has shown that for the arrangement of 4 triangles having a common vertex making up a quadrilateral in which looping is fully developed the field vanishes everywhere and is thus an eigensolution. It is also clear that this solution will exist even if other iron elements are present, and for each such arrangement one eigenvalue of C vanishes. Returning to the large but finite μ case it is also clear that such eigensolutions may be excited when μ increases. This would explain why H is no longer inversely proportional to χ. Fortunately, as observed in actual cases, the field in air is not affected by this eigensolution and quadrilateral prisms may not cause this problem. (See next section.)

5.3 Iron Element Shapes. Rectangular cross-section iron elements can be used to cure looping but they introduce other problems. At low fields, results computed using rectangles are always less than expected. Although the results do converge as the number of elements is increased the errors are still large when the maximum number of elements is used. In general, quadrilateral cross section elements only give correct results if the normals to the faces of the elements approximately follow the direction of the flux. It appears also that triangles consistently give the correct answer because the meshes of triangles used have normals to faces in many directions.

Meshes of right triangular prisms can give poor results when all the axes of the prisms are in the same direction, i.e. when the end planes of the prisms are all parallel. To overcome this difficulty the program was modified to use prisms in any orientation. This has proved a reasonable solution.

The way of correcting the problem is clear. Tetrahedral iron elements should cure problems found using prisms and perhaps linear variation may further improve the solution.

6. DEVELOPMENT WORK.

6.1 Triangular Mesh Generator for Polygrams. In the present production version of GFUN, triangular meshes in iron regions are generated by mapping a general quadrilateral in real space on to a unit square in a pseudo space, subdividing into regular triangles, and then mapping back into real space to obtain the coordinates of the irregular triangular mesh. Annular sections are treated in a similar fashion.

A new mesh generator[13] has been developed to cater for regions of more general shape using a different method. The shape handled is a general polygram each side of which can be an arc of a circle. The user specifies the boundary of the polygram and the total number of triangles into which he wants it to be subdivided. The method is to calculate the size of a regular right angled isosceles triangle, the given number of which would fill the area of the polygram. A regular triangular mesh of such triangles is superimposed over the polygram and nodes in this mesh which are near to the boundary are moved to coincide with the boundary. Finally, in an iterative relaxation process, the coordinates of the internal nodes are adjusted to spread the distortion as evenly as possible.

This option will be introduced in the production version of GFUN in the near future. In implementing this mesh generator, a new language (POLLY) which enables users to define polygrams with the minimum amount of information has been developed.

6.2 Tetrahedral Iron Elements. This element shape is most convenient for fitting awkward corners and can be combined with the earlier prismatic elements to give prisms with obliquely sliced ends, so that the axes may follow the field round a corner.

A routine has been written to evaluate the coefficients from a tetrahedral element and the results checked by splitting a prism into 3 tetrahedrons. The formulation is readily adaptable to any polyhedral element. It is given in Section 11.1.

6.3 Linear Variation of Magnetisation. The idea of this approach is to replace the assumption of constant magnetisation within an element by an assumption of magnetisation which is a linear function of its values at the corners of the element. For implementing this idea the tetrahedron is the natural element shape since the four corners give just the number of constraints required to determine a linear function.

Since the magnetisation, but not however its derivatives, is now continuous, the method would seem to allow the model more accurately to represent reality. Also for a given division of space there are nearly always fewer nodes than elements, an unbounded medium having only 1/6 node per tetrahedron.

Formal closed expressions for the field of a linearly magnetised tetrahedron[14] have been obtained. However the expressions are singular on edges and corners, and although these singularities cancel out at internal points, at external boundaries they correspond to physical regions of saturated iron near surfaces of high curvature. Before the idea can be implemented these difficulties must be overcome.

The possibilities for doing this are, firstly: simply to radius all corners and edges, secondly: to place all the nodes internally and deal with the omitted region by extrapolation, or thirdly: to use some function other than a linear one to represent an element with external edges.

6.4 Use of Minicomputer for Graphics and Some Analysis. At present GFUN runs in the Rutherford Laboratory IBM 360/195. The operating system is aimed at optimising batch use of the computer and does not allow interactive jobs to share memory on a time basis. Therefore when the user is thinking, or typing, a large amount (200 Kbytes) of memory is occupied inactively. This problem will be relieved by separating GFUN tasks into those which do not demand a large fast machine and those which do. These simple tasks will be implemented on a minicomputer which will have a link to the main computer. When substantial tasks are requested, a job will be launched into the batch of the main computer via the link, and the results will be returned in the same way. Tasks which can clearly be implemented on the minicomputer are data definition, display and editing, file management, and display of results. Tasks such as solving a large set of non-linear equations will clearly involve the main computer. Tasks of intermediate complexity such as calculating the field at several points will be the subject of some experiment. A possible course of action is to ask the main computer to calculate the field in a regular mesh for subsequent interpolation, or to fit a function to such data for subsequent evaluation.

The advantages of such a system would be as follows:

1. It would be easy to accommodate several simultaneous users. The computer available (GEC 4080) is aimed at such real-time use.

2. The program would be available continuously without using the main computer memory except when necessary, via the batch.

3. Any new graphics device which became available in the future could be easily incorporated, as the graphics package is virtually device independent.

4. It will be easier to experiment with special purpose hardware micro-processors as they become available (eg. mathematical functions, etc.).

5. The majority of the subroutines will be in easily transportable ANSI standard Fortran.

6. Personal storage of magnet files on magnetic tapes (or possibly 'floppy' disks) will be convenient.

The only disadvantage is that some tasks which could possibly be expected to give rapid response may now incur some delay. If optimum use is made of the main computer, once access is obtained, this may be acceptable. It should be pointed out that already some tasks are impossible interactively because the computing time is too great.

Advantage is being taken of this development to re-design the data structures of the program and to make the software as modular as possible, so that future developments (such as more powerful mesh generators, etc.) can be incorporated with minimum effort.

6.5 Magnet Coils of Arbitrary Shape. Work is proceeding on a set of subroutines to find the magnetic field from a coil of arbitrary shape composed of bars of rectangular section which may be either straight or curved in the arc of a circle. Each bar has a local coordinate system associated with it, in which its dimensions are specified. These are then transformed into a general coil coordinate system by using Eulerian angles and computing the transformation matrix.

The data are checked for errors such as non-continuity and bars sharing a common volume.

7. FUTURE IDEAS

7.1 Alternative Methods of Solution - Integral Boundary Method. Using Green's theorem an harmonic or biharmonic differential equation can be transformed to a surface integral equation.[16] To calculate magnetic fields an integral equation for the scalar potential and its normal derivative to the surface must be solved over all the boundary surfaces between regions of different permeability. The method can only be strictly applied to linear problems; however non-linear problems could possibly be solved by a perturbation technique.

The advantages of this method are that scalar potential can be used in 3D calculations and that only the surfaces of iron regions need be defined in linear problems. A two-dimensional computer code based on this method has been written and is being tested. First results look very encouraging.[20]

7.2 Minimisation Algorithms. As mentioned in Section 2.3.4, it is intended to use some of the standard algorithms for minimising non-linear functions which combine guaranteed convergence with rapid termination. As is usual with non-linear problems, it is not possible in advance to say which of several methods will give best results. Existing Fortran routines assume that the number of independent variables is small enough for main memory to be used for all storage. Several of these will be tested on small problems. If any method appears effective it will be implemented as a Fortran routine which uses a disc for bulk storage.

Generalised linear methods of block successive over-relaxation have been tried. The members of the block are chosen to give a dominant sub-set which may guarantee convergence.

7.3 Eddy Currents. Following the development of an integral equation technique for static magnetic fields it was decided to investigate the suitability of a similar method for eddy current problems. The method currently under study[22] involves a combination of GFUN for 3D static fields with a time stepping program using vector potential for the induced currents. The conduction regions are subdivided into elements of constant current density and magnetisation so that the vector potential can be expressed as a linear combination of current sources and magnetisation sources.

7.4 Dynamic Mesh Generation. There are several ideas for dynamically adjusting the mesh as the calculation proceeds. It is hoped that these can be developed in the course of time. The aim is to subdivide the mesh where fine detail is needed, so that the problem may be solved as economically as possible.

8. CONCLUSIONS

The results given in Section 3 demonstrate that the 3D program is capable of predicting the magnetic field for a wide variety of magnets. The accuracy that can be achieved depends upon the complexity of the magnet geometry. The shape of the fields can be predicted to better than 1%. However, due to the limitations of the present program discussed in Section 5, the predictions of field magnitude can vary in accuracy. For example in the case of the VEC magnet discussed in Section 3.1 there were insufficient prism elements to adequately represent both the complicated pole shape and the return yoke.

The constant magnetisation model of a ferromagnetic material as used in the present version of the program has been extended as far as possible and is now limited by the size and speed of the computer.

Clearly much remains to be explored, for example, higher order representations of the magnetisation and the use of tetrahedral elements should enable the program to be used for more complicated systems.

9. REFERENCES

1. M J Newman, C W Trowbridge, L R Turner. GFUN: An Interactive Program as an Aid to Magnet Design. RPP/A94 (Rutherford Laboratory 1972)
2. C W Trowbridge. Progress in Magnet Design by Computer. RPP/A92 (Rutherford Laboratory 1972)
3. L R Turner. Direct Calculation of Magnetic Fields in the Presence of Iron, as Applied to the Computer Program GFUN. RL-73-102(Rutherford Laboratory 1973)
4. C J Collie, N J Diserens, M J Newman, C W Trowbridge. Progress in the Development of an Interacting Computer Program for Magnetic Field Design and Analysis in Two and Three Dimensions. RL-73-077 (Rutherford Laboratory 1973)
5. H I Rosten. A Method for the Calculation of the Magnetostatic Field from a Wide Class of Current Geometries. RL-74-077 (Rutherford Laboratory 1974)
6. C J Collie. KURLY: A Program for Computing the Magnetic Fields of 2-Dimensional Arrays of Conductors. RL-73-032 (Rutherford Laboratory 1973)
7. B Colyer. The Geometry of Constant Perimeter Dipole Windings. RL-73-143 (Rutherford Laboratory 1973)
8. Finesse Abstract. CNME/AS/18. National Research & Development Corporation.
9. M J Newman. Provisional title - DSKSOL - A Fortran package for solving linear equations with a large dense matrix using direct access disk storage. (To be published as a Rutherford Laboratory Report)
10. M J Newman. Provisional title - SECANT - A Fortran package for solving large sets of non-linear equations using the secant method and disk storage. (To be published as a Rutherford Laboratory Report)
11. J H Coupland, K J Howard. A Discussion of Some Results from the First Magnetic Field Survey of the Harwell Variable Energy Cyclotron, April - May 1964. NIRL/M/78 (Rutherford Laboratory 1965)
12. A S L Parsons. Private communication.
13. J F Marshall. GFUN Mesh Generator. RL-74-108 (Rutherford Laboratory 1974)
14. C J Collie. Magnetic Field of a linearly Magnetised Tetrahedron.CAG 74/9(Rutherford Laboratory 1974)
15. C J Collie, C W Trowbridge.GFUN Linear Variation of Magnetisation.RL-74-132(Rutherford Laboratory 1974)
16. M A Jaswon. Integral Equation Methods in Potential Theory, 1. Proc. Roy. Soc. SerA.275, 23-32(1963)
17. A Proposal to Build a 14 GeV Electron-Positron Colliding Beam Facility - EPIC. RL-74-100 (Rutherford Laboratory 1974)
18. A G Armstrong, J Simkin, C W Trowbridge. Shims for the EPIC Prototype Dipole Magnet (Calculations) RL-75-013 (EPIC/MC/69) (Rutherford Laboratory 1975)
19. Ch. Iselin. Private communication.

20. J Simkin, C W Trowbridge. The Integral Boundary Method Applied to the Solution of Magnetostatic Problems. (To be published as a Rutherford Laboratory Report)

21. D E Lobb. Computer Calculations of the Three Dimensional Magnetic Fields Produced by Conventional Quadrupole Magnets. (These Proceedings)

22. J Simkin, C W Trowbridge. Eddy Current Computer Program using an Integral Equation Formulation. (To be published as a Rutherford Laboratory Report)

10. ACKNOWLEDGEMENTS

The authors are indebted to the following:

D Andrews for refinements to the mesh generator; D S Barlow for help in producing the paper; D E Baynham for measurements on the AC5 magnet; C H Booth for measurements on the XM14 magnet; D Bryan for working on a general coil description program; J H Coupland for measurements on the VEC magnet; Mrs E L Dawson for preparing the typescript; T Docker for rewriting the file handling system; and the staff of the Rutherford Laboratory Computer and Photographic Sections.

11. APPENDIX

11.1 Tetrahedral Iron Elements

The magnetostatic potential of the element Φ is:

$$\Phi = -1/4\pi \iiint (\underline{M}.\underline{r})/r^3 \, dV$$

where the magnetisation vector $\underline{M}$ is constant by hypothesis, and $\underline{r}$ is the displacement from the field point. By Gauss's theorem this volume integral can be re-written as the surface integral:

$$\Phi = +1/4\pi \iint (\underline{M}.\underline{dS})/r.$$

For a polyhedron the direction of $\underline{dS}$ is constant over any one face. Calling this direction ζ, M_ζ is a constant so:

$$\Phi = \sum_{\text{faces}} \frac{M_\zeta}{4\pi} \iint \frac{dS}{r}.$$

The integral is now amenable to Gauss's theorem in its 2-dimensional form and is re-written:

$$\Phi = \sum_{\text{faces}} \frac{M_\zeta}{4\pi} \int \frac{\underline{r}.\underline{ds}}{(r+|\zeta|)}.$$

Again, for a polyhedron, the direction of $\underline{ds}$ is constant along any one edge, and the component of $\underline{r}$ normal to the edge is also constant, say η. Thus:

$$\Phi = \sum_{\text{faces}} \sum_{\text{edges}} \frac{M_\zeta}{4\pi} \int \frac{\eta d\xi}{(r+|\zeta|)}$$

in which $\xi\eta\zeta$ is a set of coordinates with ξ along an edge and ζ normal to a face.

The field components in the $(\xi\eta\zeta)$ space are now obtained by differentiating Φ. The results are:

$$H_\xi = \sum_{\text{faces}} \sum_{\text{edges}} \frac{M_\zeta}{4\pi} \eta \left[\frac{1}{(r+|\zeta|)}\right]_{\xi_1}^{\xi_2}$$

$$H_\eta = \sum_{\text{faces}} \sum_{\text{edges}} \frac{M_\zeta}{4\pi} \left[\log (r+\xi) - \frac{\xi}{(r+|\zeta|)}\right]_{\xi_1}^{\xi_2}$$

$$H_\zeta = \sum_{\text{faces}} \sum_{\text{edges}} \frac{M_\zeta}{4\pi} \left[\frac{|\zeta|}{\zeta} \arcsin \left(\frac{\xi\eta}{q(r+|\zeta|)}\right)\right]_{\zeta_1}^{\xi_2}$$

$$(q^2 = \zeta^2 + \eta^2)$$

The H_ζ terms for a particular face sum to the solid angle subtended by the face at the field point. The $(\eta, -\xi)$ terms in fact cancel on summation and could have been removed by imposing a condition on the divergence of the vector used in the surface integral. Further details may be found in[14].


rutherford
laboratory
reproduction
section